Proc. Natl. Acad. Sci. USA
Vol. 79, pp. 3523–3526, June 1982
Biophysics

NMR chemical shift imaging in three dimensions

(*in vivo* biochemistry/^{31}P imaging/metabolite mapping)

T. R. BROWN*, B. M. KINCAID*, AND K. UGURBIL†

*Bell Laboratories, Murray Hill, New Jersey 07974; and †Department of Biochemistry, Columbia University, New York, New York 10032

Communicated by John J. Hopfield, March 10, 1982

ABSTRACT **A method for obtaining the three-dimensional distribution of chemical shifts in a spatially inhomogeneous sample using Fourier transform NMR is presented. The method uses a sequence of pulsed field gradients to measure the Fourier transform of the desired distribution on a rectangular grid in (k,*t*) space. Simple Fourier inversion then recovers the original distribution. An estimated signal/noise ratio of 20 in 10 min is obtained for an "image" of the distribution of a 10 mM phosphorylated metabolite in the human head at a field of 20 kG with 2-cm resolution.**

There has been considerable recent interest in obtaining images from animals and humans by using NMR spectroscopy (1–9). A recent review (10) summarizes and compares many of these methods. With few exceptions (11, 12), previous workers have used protons for NMR imaging because of signal/noise (S/N) considerations and because the proton signal from tissue comes predominantly from water and therefore is at a single resonant frequency. The latter condition is necessary because most imaging methods are unable to cope with a distribution of resonant frequencies. We present here a method that determines the frequency (chemical shift) distribution at each spatial point with an optimum S/N ratio. As shown below, by suitably pulsing magnetic gradients across a specimen contained within a single pick-up coil, an "image" can be constructed consisting of high-resolution NMR frequency distributions averaged over the resolution volume. This is possible because a pulsed gradient encodes positional information in the initial phases of the free induction decay but does not affect the resonant frequency distribution in space after the gradient has been turned off. Thus, by sampling the free induction decay after a gradient pulse, information about spatial variation can be separated from information about frequencies. The net effect is to measure the Fourier transform of the spatial and frequency distribution function of the spins. This is then inverted to obtain the spatial distribution of frequencies (chemical shifts) over the sample.

THEORY

We wish to observe an object that has a spatially varying frequency distribution. Let $\rho(\mathbf{x},\delta)$ be the distribution of chemically shifted frequencies, δ, at the point $\mathbf{x}$ in such an object, as shown in Fig. 1. If we apply a rf pulse in the presence of a uniform static field, $H_o\hat{z}$, the resultant free induction decay (FID) will be

$$S(t) = \int \rho(\mathbf{x},\delta)e^{i\delta t}d\mathbf{x}d\delta,$$

assuming the entire object is excited and detected uniformly. Obviously, in this case, there is no way to recover the original distribution $\rho(\mathbf{x},\delta)$ because the spatial information is inextricably mixed with the frequency information. If, however, in addition to the static uniform field, $H_o\hat{z}$, we add a slowly (compared with the resonant frequency of the spins) varying linear gradient, $[\mathbf{G}(t)\cdot\mathbf{x}]\hat{z}$, as shown in Fig. 1, how will this affect the FID? Under these conditions, the phase of each spin at time t after a rf pulse will depend on both $\mathbf{x}$ and δ as its instantaneous frequency is now given by $\frac{d\phi}{dt} = \gamma H_T(t)$, where γ is the gyromagnetic ratio for the species under observation and $H_T(t) = [H_o + \mathbf{G}(t)\cdot\mathbf{x}](1 + \varepsilon)$. Here we have just augmented the externally applied field, $H_o + \mathbf{G}(t)\cdot\mathbf{x}$, by $(1 + \varepsilon)$ to take into account the electronic shielding that causes the chemical shift effect. The chemically shifted frequencies, δ, are $\gamma(1 + \varepsilon)H_o$. Thus, $\frac{d\phi}{dt} = \delta + \gamma(1 + \varepsilon)\mathbf{G}(t)\cdot\mathbf{x} = \delta + \gamma\mathbf{G}(t)\cdot\mathbf{x}$ to a very high accuracy since $\varepsilon \approx 10^{-5}$ and the ratio of the gradient to the main field strength is also $\approx 10^{-5}$. Integrating our final expression for $\frac{d\phi}{dt}$, we obtain

$$\phi(\mathbf{x},t) = \delta t + \gamma\int_0^t \mathbf{G}(\tau)\mathbf{x}d\tau.$$

If we let

$$\boldsymbol{\kappa}(t) = -\gamma\int_0^t \mathbf{G}(\tau)d\tau,$$

then the observed FID will be

$$S(t) = \int \rho(\mathbf{x},\delta)e^{i[\delta t - \boldsymbol{\kappa}(t)\cdot\mathbf{x}]}d\mathbf{x}d\delta.$$

This is just the Fourier transform of $\rho(\mathbf{x},\delta)$ in both space and frequency. Let $\bar{\rho}(\boldsymbol{\kappa},t)$ be this transform. Our final answer is then

$$S(t) = \bar{\rho}[\boldsymbol{\kappa}(t),t].$$

This result simply states that the observed FID samples the Fourier transform, $\bar{\rho}$, of the original distribution along a curve in $(\boldsymbol{\kappa},t)$ space described by the equation

$$\frac{d\boldsymbol{\kappa}}{dt} = -\gamma\mathbf{G}(t).$$

Consider the case in which $\mathbf{G}(t)$ is merely a constant, $\mathbf{G}$. Then

$$S(t) = \boldsymbol{\rho}(-\gamma\mathbf{G}t,t).$$

So, by measuring the FID in the presence of the gradient $\mathbf{G}$, we have measured the Fourier transform of the desired distribution function along the straight line $\mathbf{k} = -\gamma\mathbf{G}t$ in $(\mathbf{k},t)$ space. If it were possible to measure along all such lines, we could reconstruct the original distribution as its transform would be known everywhere. It is clear, however, that we are limited in k space by the maximum possible gradient, G_{max}. In addition, the nonuniform sampling in k space is usually inefficient in terms of S/N ratio as a higher density of samples near the origin

The publication costs of this article were defrayed in part by page charge payment. This article must therefore be hereby marked "*advertisement*" in accordance with 18 U. S. C. §1734 solely to indicate this fact.

Abbreviations: S/N, signal/noise; FID, free induction decay; Fru-6-*P*, fructose 6-phosphate; *P*-creatine, phosphocreatine.

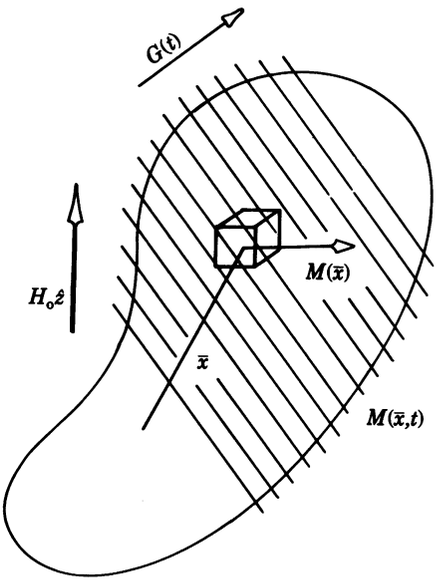

FIG. 1. An object that has a spatially varying chemical shift distribution in a magnetic field gradient. $M(\mathbf{x},t)$ is the local magnetization density at point $\mathbf{x}$ at time t and is equal to $\int \rho(\bar{\mathbf{x}},\delta)e^{i\phi(\mathbf{x},\delta,t)}d\delta$. Lines indicate constant frequency at time t. The total signal, S(t), is the integral of $M(\mathbf{x},t)$ over the sample volume.

than needed results from the need to sample adequately near t_{max}. This sampling problem has been reviewed by Klug and Crowther (13) in a theoretical analysis of different reconstruction algorithms.

An easier method would be to measure the transform on a rectangular mesh in $(\mathbf{k},t)$ space, eliminating the nonuniform sampling problem. To accomplish this, we simply turn off the gradient after a short time, t_0. The FID now is

$$S(t) = \bar{\rho}(-\gamma \mathbf{G}t,t); \qquad t < t_0$$
$$= \bar{\rho}(-\gamma \mathbf{G}t_0,t); \qquad t > t_0.$$

Thus, for times $t > t_0$, we are sampling $\bar{\rho}$ parallel to the t axis with $\mathbf{k}$ equal to $-\gamma \mathbf{G}t_0$.

By measuring $S(t)$ at various values of $\mathbf{G}t_0$ (set by the size of the object and the degree of spatial resolution desired), we will have sampled the Fourier transform of the original distribution inside a box limited by the maximum values of $\mathbf{G}t_0$ and by the maximum and minimum sampled times. If we then Fourier transform these values to obtain a filtered version of the original distribution, how closely will it agree with the original? Since the k-space sampling can be uniform and extended to large k, its transform will have only the well-known errors associated with aliasing or frequency foldover and the minimum resolution of a finite sampling period. In this connection, we should point out that in this method all the eigenvalues discussed by Klug and Crowther are 1, thus leading to a reconstructed image in which all the data are used with no loss of high spatial frequencies. The transform in time has, in addition to these, the errors coming from the loss of information for $t < t_0$. This attenuates broad frequency features of width $\lesssim 1/t_0$ Hz. This should not be serious as t_0 can be $\approx$1 ms or less in most cases. For example, for ^{31}P (γ = 1,720 Hz/G), a gradient strength of 3 G/cm, pulsed for 1 ms, would correspond to a resolution of 1 mm in the sample.

Before turning to a specific example, the S/N ratio in general should be considered. Perhaps the simplest way to determine the overall S/N ratio is to consider the case in which only a single resolution element is present in the coil at some arbitrary location. Then, as various gradients are applied, the same frequency distribution is observed in the coil each time but with various initial phases. Assume the noise is dominated by coil losses and is independent of the signal. Under these conditions, the Fourier transform in k space simply untangles the various initial phases so that the different measurements can be added together coherently. Thus, after n different measurements, the signal will be n times larger while the noise will only increase as $n^{1/2}$. The S/N ratio is then $n^{1/2}$ times the S/N ratio for a single pulse. This is, of course, just the expected increase due to the longer observation time. Therefore, since the system is linear and the series of operations on each individual volume element is unchanged if the entire specimen is present, the S/N ratio for the entire specimen is equal to that which would be obtained for each element separately. Hence, the only loss over normal high-resolution Fourier transform NMR is that due to the smaller filling factor occupied by the spatial resolution element. This appears to us to be the optimum possible for imaging methods of this type (i.e., using NMR).

To demonstrate the feasibility of this method, we have applied it to a simple one-dimensional phantom consisting of two parallel cylinders, one containing P_i and the other containing fructose 6-phosphate (Fru-6-*P*). The demonstration was restricted to one dimension because of computational size limitations; with sufficient memory, three dimensions could be done with the same algorithms.

METHODS

The data were taken at 145.7 MHz on a Bruker 360 HX spectrometer that had been modified to allow the room temperature y-gradient shim coils to be pulsed by the computer controlling the spectrometer through a digital-to-analog converter. The sample consisted of two 100-μl pipettes, one filled with 0.2 M P_i and the other filled with 0.2 M Fru-6-*P*, placed approximately at the center of a standard 10-mm sample tube. The ends of the pipettes were sealed and the rest of the sample tube was filled with water to improve the magnetic field homogeneity. The pipettes were 1.5-mm inside diameter and their centers were separated by $\approx$2.5 mm. The sample was rotated in the magnet until the maximum effect of a static y gradient was observed. We estimate the plane between the cylinders to be aligned with the y-gradient axis to $\pm$15°. The volume of each pipette sampled by the coil is $\approx$20 μl (i.e., 1 cm in the vertical direction).

Data were taken at 64 different values of the y gradient in the following manner. A 30° rf pulse was applied simultaneously with turning on the gradient and initiation of data collection. After 5 ms, the gradient was removed and the remainder of the FID was sampled. This was repeated 10 times for each gradient value after which the FID was stored and the computer initiated the same sequence for the next gradient value. Each gradient step corresponded to 0.1 G/cm. Total time for data accumulation was 2.3 min.

After acquisition, the FIDs were zeroed during the first 5 ms and then Fourier transformed with respect to time to obtain a frequency distribution and the region of interest around the two resonances was selected. The spectra were then Fourier transformed again with respect to the gradient values.

RESULTS

A two-dimensional plot of the doubly transformed data is shown in Fig. 2. The horizontal axes are space and frequency. The spatial scale was calculated from the known strength of the gradients and corresponds to 0.3 mm per point. The origins of

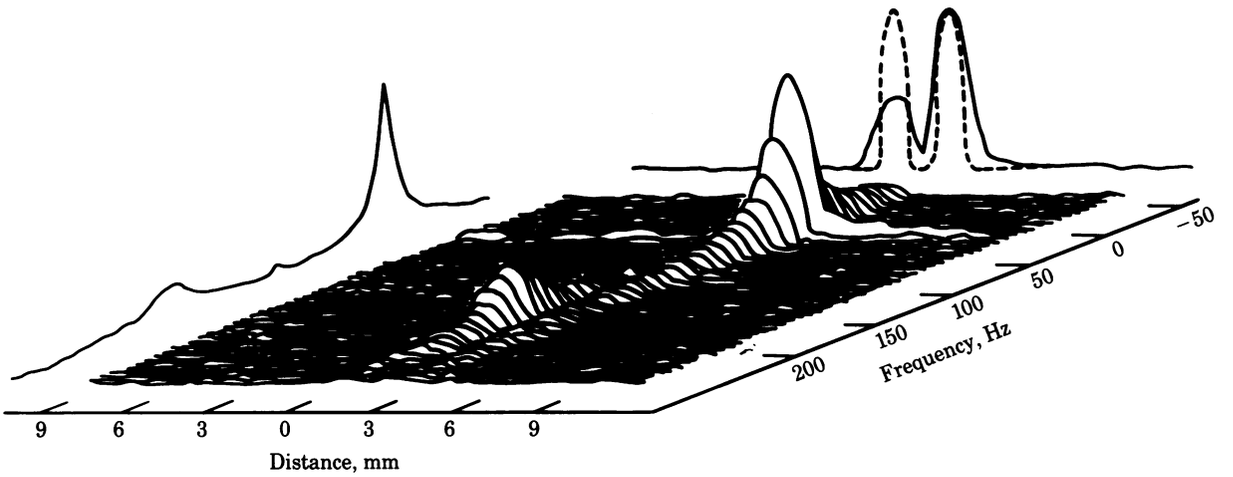

FIG. 2. Distribution in one spatial dimension and frequency (chemical shift) of a phantom consisting of two parallel 1.5-mm (inside diameter) cylinders spaced 2.5 mm apart. Solid lines at the left and rear are sums over space and frequency, respectively. The dotted line is the theoretically expected spatial profile normalized in height to the larger peak.

both axes are arbitrarily chosen. The lower wider peak is from Fru-6-*P*, the other is from P_i. To visualize directly the spatial distributions one would like to sum the data at a given point over frequency. Unfortunately, because the initial 5 ms of the FID was zeroed, a sum of just the real part must necessarily give zero. To overcome this, we have used the amplitude of each point—i.e., the square root of the sum of the squares of the real and imaginary parts—as the vertical displacement in the figure. The solid curves at the edges are the sums over space and frequency. The dashed curve is the theoretically expected spatial profile normalized to the P_i peak in amplitude and position. The Fru-6-*P* intensity is lower than that of the P_i because its extra width in frequency due to the higher viscosity of the 0.2 M Fru-6-*P* solution causes proportionately more of its intensity to be lost when the first 5 ms of the FID is zeroed.

We have also simulated this technique on a computer by using theoretically calculated FIDs in both one and two dimensions. The one-dimensional simulations agree quite well with our data. The two-dimensional simulation is shown in Fig. 3 for two compounds in two different regions. We have plotted the two peak amplitudes as a function of space together with the sum of all frequencies on the lower graph. As expected, we can resolve the two separate components even in the case in which the physical regions overlap.

DISCUSSION

To estimate reasonable resolutions and imaging times in a three-dimensional object such as an animal or a human, we use the fact that the S/N ratio expected in the high-resolution chemical shift spectrum from a given volume in a three-dimensional sample obtained by this method is the same as that obtained if only that region were contributing signal to the pickup coil. In the case of a small animal or an isolated organ, such as a perfused heart, which have been studied in static fields up to 80 kG, we can estimate S/N ratios from the observed spectra.

For example, ≈2 ml of skeletal muscle in a static field of 60 kG gives after one 90° pulse a S/N ratio of 20 for the 10-Hz-wide resonance due to the phosphocreatine (*P*-creatine) present at 20 mM (14). Spin echo measurements on these muscles give a T_2 of 0.25 s for *P*-creatine (unpublished results). Since the 10-Hz-wide resonance rings down in 50 ms (T_2^{app} = 30 ms), if there were some way to sample different k values while simultaneously refocusing the spins, we would be able to measure five or so different values in the T_2 time of 250 ms. This can be accomplished by pulsing the gradient coils, in each 50-ms interval, in such a way that $\mathbf{G}(t)$ is an antisymmetric function with respect to the middle of the interval where the refocusing 180° pulse occurs. Then by varying the strength or direction of $\mathbf{G}(t)$ in each interval, we can measure a different k value. In this scheme, corrections are needed for the effects of the true T_2 decay on the Fourier components measured in the later intervals. As

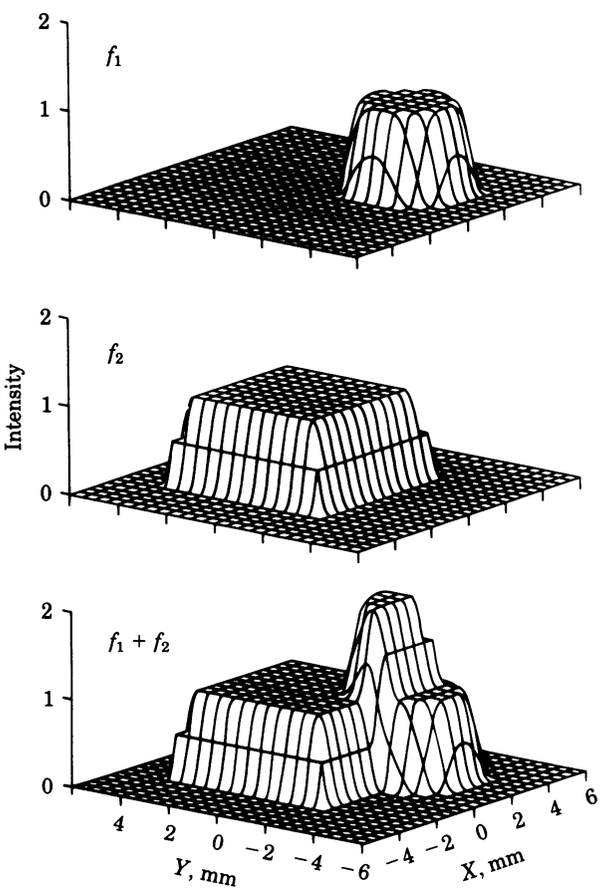

FIG. 3. Computer simulation of a two-dimensional object that has spatially varying chemical shifts.

these T_2s are known, such corrections should be straightforward. To sample again, one must now wait a time on the order of T_1, which is 2.5 s for *P*-creatine under these conditions (14). We can then reasonably expect to measure one k value in 0.5 s on the average.

Because of the fast repeat times used, the S/N ratio of the entire muscle for a single pulse is ≈10 instead of the 20 mentioned above. For a volume of 2 mm^3, it would be 10^{-2} for one pulse. If 10^3 k values are desired (resolving the muscle into regions 10 × 10 × 10 on each side), then 500 s are required for their accumulation. Each resolution volume would then be 2 mm^3. The S/N ratio of each of the 2-mm^3 resolution elements after 500 s would be 30 $[(10^3)^{1/2}]$ times the S/N ratio of that volume in a single pulse, or 0.3, obviously too small to be useful. However, by adding 100 such volumes together, a S/N ratio of 3 would be achieved from a volume of 0.3 ml. This volume, if it were a cube, would be 6 mm on a side. But it need not be a cube, as any of the three-dimensional elements can be added together (for example, if one wishes to observe a long cylinder or a thin disk).

Scaling such estimates down to 20 kG and large specimens can be done by reducing the S/N ratio as the field to the 3/2 power. A further reduction is needed if an entire specimen is to be observed as the pickup coil must be made larger, reducing the S/N ratio linearly with its diameter.‡

First, we estimate for one pulse the S/N ratio from a 10 mM phosphorylated metabolite in a 2-ml volume inside a human head (assumed to be 20 cm on a side) in a 20-kG static field, using the previous S/N ratio of 20 for 20 mM *P*-creatine in 2 ml of muscle. Then, for one pulse, we have

$$\mathrm{S/N} = 20 \times \frac{10\ \mathrm{mM}}{20\ \mathrm{mM}} \times \left(\frac{\text{new field}}{\text{old field}}\right)^{3/2} \times \left(\frac{\text{old coil radius}}{\text{new coil radius}}\right)$$

or

$$20 \times \frac{10\ \mathrm{mM}}{20\ \mathrm{mM}} \times \left(\frac{20}{60}\right)^{3/2} \times \left(\frac{2\ \mathrm{cm}}{20\ \mathrm{cm}}\right) = 0.2 \text{ or } 0.1/\mathrm{cc}.$$

If the same relative resolution of 10 × 10 × 10 is desired and we assume the same sort of line widths as in skeletal muscle, in 500 s we again would have measured 10^3 k values. The resolution volume now is ≈2 × 2 × 2 ml, so the S/N ratio in this volume is 0.1 × 30 × 8 = 24. If a resolution of 1 cm is desired, then 8 times as many k values are needed, requiring 1 hr of data accumulation. In this case, the S/N per resolution volume of 1 ml is 0.1 × 90 × 1 = 9.

Although estimates of this sort must be regarded with some caution until experimentally verified, they are usually correct within a factor of 2 or so, provided there are no serious corrections due to rf skin depth effects. At 20 kG, the resonant frequency of ^{31}P is 35 MHz, which corresponds to a skin depth of ≈10 cm in an aqueous solution of physiological salinity (100 mM). This will cause some phase distortion of the signals originating near the center of the head but not more than a factor of 2 loss in their amplitude. As each volume element of the sample can be phased separately as required, it should be no problem to correct the phases of the internal regions if necessary. Thus, we feel that it is reasonable to expect that images of the major phosphorylated metabolites in intact animals and humans can be obtained in tens of minutes with spatial resolutions of a few centimeters and S/N ratios of ≈10. In addition, the use of surface coils (15) to image only regions of interest will reduce the number of different k values needed to recover an image and therefore result in faster data acquisition.

With regard to human observations, safety considerations are quite important. As far as is known, brief exposures to static fields of 20 kG cause no harmful effects. The average rf power levels absorbed would be less than a few tenths of a watt delivered to the entire head. As this is less than 1% of the resting heat generated in the head, it seems unlikely to cause any difficulties. Another consideration is the pulsed gradients required. As mentioned above, 3 G/cm for 1 ms corresponds to a resolution of 1 mm, far smaller than anything required. A more realistic gradient is 0.3 G/cm for 1 ms, corresponding to 1-cm resolution. If this is applied across 20 cm for 1 ms, then a time-varying field of 6 kG/s would be applied to the object. Again, this is within accepted limits (16).

In conclusion, we have presented a method for obtaining with high S/N ratio the chemical shift distribution in a three-dimensional object. The technique appears to be of general applicability and is expected to produce an image of a phosphorylated metabolite of 10 mM concentration in a human head in a 20-kG static field in 10 min with a resolution of 2 cm and a S/N ratio of 10–20.

‡ This reduction occurs because the amount of flux from a magnetic dipole that intersects a coil of radius r decreases inversely with $1/r$.

1. Lauterbur, P. C. (1973) *Nature (London)* **242**, 190–191.
2. Hinshaw, W. S. (1976) *J. Appl. Phys.* **47**, 3709–3721.
3. Kumar, A., Welti, D. & Ernst, R. R. (1975) *J. Magn. Res.* **18**, 69–83.
4. Mansfield, P. & Pykett, I. L. (1978) *J. Magn. Res.* **29**, 355–373.
5. Hoult, D. I. (1979) *J. Magn. Res.* **33**, 183–197.
6. Brunner, P. & Ernst, R. R. (1979) *J. Magn. Res.* **33**, 83–106.
7. Doyle, F. H., Pennock, J. M. & Orr, J. S., *et al.* (1981) *Lancet*, 53–57.
8. Hawkes, R. C., Holland, G. N., Moore, W. S. & Worthington, B. S. (1980) *J. Comp. Asst. Tom.* **4**, 577–586.
9. Holland, G. N., Hawkes, R. C. H. & Moore, W. S. (1980) *J. Comp. Asst. Tom.* **4**, 429–433.
10. Edelstein, W. A., Hutchinson, J. M., Johnson, G. & Redpath, T. (1980) *Phys. Med. Biol.* **25**, 751–756.
11. Lauterbur, P. C., Kramer, D. M., House, W. V., Jr., & Chen, C.-N. (1975) *J. Am. Chem. Soc.* **97**, 6866–6868.
12. Bendel, P., Lai, C.-M. & Lauterbur, P. C. (1980) *J. Magn. Res.* **38**, 343–356.
13. Klug, A. A. & Crowther, R. A. (1972) *Nature (London)* **238**, 435–440.
14. Kushmerick, M. J., Brown, T. R. & Crow, M. (1980) *Fed. Proc. Fed. Am. Soc. Exp. Biol.* **39**, 1934.
15. Ackerman, J. J. H., Grove, T. H., Wong, G. C., Gadian, D. G. & Radda, G. K. (1980) *Nature (London)* **283**, 167–170.
16. Budinger, T. F. (1979) *IEEE-Trans. Nucl. Sci.* **26**, 2821–2825.